

# High-Pressure Phase Equilibrium and Raman Spectroscopic Studies on the 1,1-Difluoroethane (HFC-152a) Hydrate System

Takeshi Sugahara, Aki Endo, Hiroshi Miyauchi, Seung An Choi, Yuuki Matsumoto, Kenjiro Yasuda, Shunsuke Hashimoto, and Kazunari Ohgaki\*

Division of Chemical Engineering, Department of Materials Engineering Science, Graduate School of Engineering Science, Osaka University, 1-3 Machikaneyama, Toyonaka, Osaka 560-8531, Japan

**S** Supporting Information

**ABSTRACT:** High-pressure phase equilibrium relations of the 1,1-difluoroethane (HFC-152a) + water binary system were investigated in a temperature range of (275.03 to 319.30) K and a pressure range up to 370 MPa. Four three-phase coexisting curves of hydrate + aqueous + gas phases, hydrate + HFC-152a-rich liquid + gas phases, hydrate + aqueous + HFC-152a-rich liquid phases, and aqueous + HFC-152a-rich liquid + gas phases originate from the quadruple point of hydrate + aqueous + HFC-152a-rich liquid HFC-152a + gas phases located at  $(288.05 \pm 0.15)$  K and  $(0.44 \pm 0.01)$  MPa. The structure of HFC-152a hydrate remains structure I (s-I) in the pressure range up to 370 MPa. Raman spectra of the HFC-152a molecule in the HFC-152a hydrate indicate that the HFC-152a molecules occupy only large cages of s-I HFC-152a hydrate in the presence of completely vacant small cages at a pressure up to 370 MPa.

## INTRODUCTION

Gas hydrates are crystalline substances composed of the guest species and the cages that are constructed by hydrogen-bonded water molecules. Structure I (s-I) is one of the common hydrate structures.<sup>1</sup> The s-I hydrate has two small cages (pentagonal dodecahedron ( $S^{12}$ ), hereafter, S-cages) and six middle cages (tetrakaidecahedron ( $S^{12}6^2$ ), M-cages) in the unit lattice. The familiar guest species for the s-I hydrates are methane ( $CH_4$ ), carbon dioxide ( $CO_2$ ), ethane ( $C_2H_6$ ), ethylene ( $C_2H_4$ ), and cyclopropane ( $c-C_3H_6$ ). The Raman peak corresponding to the intramolecular C–H symmetric vibration mode of  $CH_4$  molecule in  $CH_4$  hydrate divides into doublet, and the peak intensity ratio corresponds to the cage–constituent ratio of s-I.<sup>2,3</sup> The  $C_2H_4$ ,  $C_2H_6$ , and  $c-C_3H_6$  molecules, which sizes are slightly larger than the void space of the S-cage, can oppressively occupy a part of the S-cage as the pressure is raised, while they cannot occupy it in a low-pressure region.<sup>4–6</sup>

Gas hydrates are versatile for possible industrial applications, for example, refrigeration, gas storage/transportation, and gas separation. Hydrofluorocarbons (HFCs) and liquefied hydrocarbons like isobutane are possible guest species for the refrigeration system using gas hydrates because of their low formation pressure. Numerous researchers have reported the equilibrium data of some gas hydrates formed at relatively low pressures.<sup>7–12</sup> 1,1-Difluoroethane (HFC-152a) is one of the largest s-I hydrate formers,<sup>1</sup> and HFC-152a has the smallest global warming potential of all HFCs.<sup>13</sup> For the HFC-152a hydrate, the three-phase equilibrium curves of (H + I + G) and (H +  $L_1$  + G) and the quadruple points of  $Q_1$  (H + I +  $L_1$  + G) and  $Q_2$  (H +  $L_1$  +  $L_2$  + G) in the temperature range of (264.72 to 288.15) K and the pressure range of (0.0495 to 0.4437) MPa have been previously reported by Kubota et al.<sup>8</sup> and Liang et al.<sup>10</sup> In addition, Kubota et al.<sup>8</sup> have reported the three-phase equilibrium curves of (H +  $L_2$  + G) and ( $L_1$  +  $L_2$  + G). The symbols of H, I,  $L_1$ ,  $L_2$ , and G

represent the hydrate, ice, aqueous, HFC-152a-rich liquid, and gas phases. There are almost no equilibrium data at a pressure higher than that of  $Q_2$ , and the Raman spectroscopic results of HFC-152a hydrate have not yet been reported.

In the present study, we have investigated the thermodynamic stability boundaries of the HFC-152a hydrate system in a temperature range of (275.03 to 319.30) K and a pressure range up to 370 MPa. In addition, the cage occupancy of the HFC-152a molecule and the pressure effect of the intermolecular O–O vibration (lattice mode) between host water molecules have been briefly discussed based on the Raman spectra in the single crystal of HFC-152a hydrate.

## EXPERIMENTAL SECTION

1,1-Difluoroethane (HFC-152a) (minimum purity in the mole fraction is 0.995) was obtained from Daikin Industries, Ltd. The distilled water was obtained from Yashima Pure Chemicals Co. Ltd. Both were used without further purification.

We used three types of high-pressure cells depending on experimental pressures. The details of high-pressure cells are given elsewhere.<sup>14</sup> The equilibrium temperature was measured within a reproducibility of 0.02 K using a thermistor probe (Takara, model: D-641) calibrated by a Pt resistance thermometer (25  $\Omega$ ) defined by ITS-90. For pressure measurements, two different pressure gauges were used depending on the experimental pressure. Up to 75 MPa, a pressure gauge (Valcom, model: VPRT) calibrated by a Ruska quartz Bourdon tube gauge was used with an estimated maximum uncertainty of 0.02 MPa. Over

**Special Issue:** Kenneth N. Marsh Festschrift

**Received:** June 2, 2011

**Accepted:** August 3, 2011

**Published:** August 22, 2011

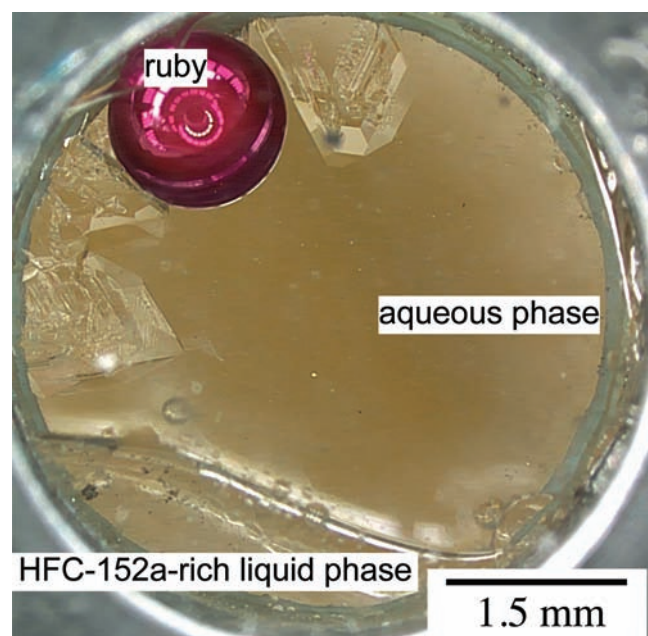


**Figure 1.** Typical photograph of the single crystals of HFC-152a hydrate at 39 MPa and 293.0 K under three-phase coexistence conditions.

75 MPa, a pressure transducer (NMB, model: STD-5000K) and digital peak holder (NMB, model: CSD-819) were used with an estimated maximum uncertainty of 2 MPa.

A desired amount of HFC-152a was introduced into the evacuated and cooled cell. A mixing magnet or a mixing ball in the cell was vibrated from the outside for agitation. The contents were pressurized up to the desired pressure by a successive supply of water. After the formation of the HFC-152a hydrate, to establish the three-phase equilibrium state, the system temperature was gradually increased, and the contents were agitated intermittently. The phase behavior of the system was observed by the charge-coupled device (CCD) camera through the sapphire window.

After the single crystal of HFC-152a hydrate was prepared on the stability boundary, HFC-152a hydrate crystals were analyzed through a sapphire window using a laser Raman microprobe spectrometer with a multichannel CCD detector (Jobin Yvon, model: Ramanor T64000). The photograph of the HFC-152a hydrate crystal at 38.7 MPa and 293.0 K is shown in Figure 1. The laser beam from the object lens irradiated every phase through the upper sapphire window. The backscatter of the opposite direction was taken in with the same lens. The argon ion laser beam of 514.5 nm and 100 mW (generation power) was condensed to a 2  $\mu\text{m}$  spot diameter. The spectral resolution was approximately 0.7  $\text{cm}^{-1}$ . All Raman spectra obtained from the hydrate single crystal can be completely distinct from those of liquid HFC-152a phase at microscopic field, under the three-phase equilibrium state of (hydrate + aqueous + HFC-152a-rich liquid phases). The powder X-ray diffraction (PXRD) pattern was measured using a diffractometer (Rigaku, model: Ultima IV) with a Rigaku D/teX ultra high-speed position sensitive detector and Cu K $\alpha$  X-ray (40 kV, 50 mA). The measurements were performed in the stepscan mode with scan rate of 10  $\text{deg} \cdot \text{min}^{-1}$  and step size of 0.02 $^\circ$ . Once the hydrate sample prepared at 281.0 K and 0.16 MPa was taken from the cell in the low-temperature room at 253 K, the sample was quenched and ground at liquid

**Table 1.** Three-Phase Coexisting Curves and Quadruple Point (Temperature  $T$ , Pressure  $p$ ) in the HFC-152a + Water Binary System<sup>a</sup>

$T/\text{K}$	$p/\text{MPa}$	$T/\text{K}$	$p/\text{MPa}$	$T/\text{K}$	$p/\text{MPa}$
H + L <sub>1</sub> + G		H + L <sub>1</sub> + L <sub>2</sub>		H + L <sub>1</sub> + L <sub>2</sub>	
275.03	0.08	288.23	2.60	306.79	183
276.10	0.09	289.40	10.51	309.40	223
276.87	0.10	290.54	19.63	309.90	226
277.79	0.11	290.48	19.02	311.52	259
278.50	0.12	290.69	20.13	314.73	315
279.16	0.13	290.68	20.55	316.01	342
279.72	0.14	290.97	23.00	319.30	370
280.23	0.15	291.21	23.93		
281.20	0.17	291.96	31.06	H + L <sub>2</sub> + G	
281.99	0.19	292.74	38.72	278.48	0.32
282.71	0.21	292.99	38.74	281.73	0.36
283.31	0.23	293.22	42.19	284.45	0.39
283.91	0.25	294.37	51.25	286.59	0.42
284.53	0.27	295.11	56.94		
285.04	0.29	295.94	64.93	L <sub>1</sub> + L <sub>2</sub> + G	
285.55	0.31	296.18	67.96	288.87	0.45
286.06	0.33	296.85	77	291.77	0.49
286.65	0.36	299.31	99	296.33	0.56
287.25	0.39	302.14	143	301.27	0.64
287.84	0.42	302.64	145		
		303.37	148		
		Q <sub>2</sub> (H + L <sub>1</sub> + L <sub>2</sub> + G)	305.07	159	
288.05	0.44	306.25	182		

<sup>a</sup> The symbols H, I, L<sub>1</sub>, L<sub>2</sub>, and G represent hydrate, ice, aqueous, HFC-152a-rich liquid, and gas phases.

nitrogen temperature for the PXRD measurement. The measurements were carried out at atmospheric pressure and  $113 \pm 2$  K using a low-temperature attachment. The PXRD pattern indexing and cell refinement were obtained with use of the Checkcell<sup>15</sup> and PowderX<sup>16</sup> programs and the initial lattice parameters<sup>1</sup> for the refinement.

## RESULTS AND DISCUSSION

The PXRD pattern of the HFC-152a hydrate formed at 281.0 K and 0.16 MPa (shown in Figure S1 of the Supporting Information) clearly indicates that the structure of HFC-152a hydrate is s-I (cubic,  $Pm\bar{3}n$ ) and the lattice parameter of the s-I HFC-152a hydrate is  $a = 1.195 \pm 0.002$  nm (measured at  $113 \pm 2$  K and atmospheric pressure). The lattice parameter obtained in the present study is similar to literature values.<sup>1</sup>

The phase equilibrium relations of the four three-phase coexistence curves are listed in Table 1 and plotted in Figure 2. The quadruple point Q<sub>2</sub> of H + L<sub>1</sub> + L<sub>2</sub> + G, which was determined by the extrapolation of four three-phase coexistence curves, is located at  $(288.05 \pm 0.15)$  K and  $(0.44 \pm 0.01)$  MPa. The three-phase equilibrium curve of H + L<sub>1</sub> + G and the quadruple point Q<sub>2</sub> are in good agreement with the data reported by Kubota et al.<sup>8</sup> and Liang et al.<sup>10</sup> The equilibrium pressures increase monotonically and moderately with temperature. The smoothness of the three-phase coexisting curve of H + L<sub>1</sub> + L<sub>2</sub> suggests that there is no structural phase transition point in the

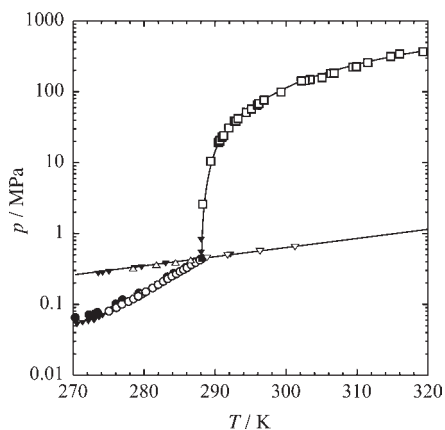


**Figure 2.** Three-phase coexisting curves of the HFC-152a + water binary system. All open symbols, present study ( $\circ$ , H + L<sub>1</sub> + G;  $\triangle$ , H + L<sub>2</sub> + G;  $\nabla$ , L<sub>1</sub> + L<sub>2</sub> + G;  $\square$ , H + L<sub>1</sub> + L<sub>2</sub>);  $\blacktriangledown$ , ref 9;  $\bullet$ , ref 11. The closed square symbols stand for the quadruple points Q<sub>1</sub> (H + I + L<sub>1</sub> + G)<sup>10</sup> and Q<sub>2</sub> (H + L<sub>1</sub> + L<sub>2</sub> + G) (present study). The symbols H, I, L<sub>1</sub>, L<sub>2</sub>, and G represent hydrate, ice, aqueous, HFC-152a-rich liquid, and gas phases.

experimental pressure range of the present study; that is, the structure of the HFC-152a hydrate remains s-I in the high-pressure region of about 370 MPa.

The HFC-152a molecule has a lot of Raman-active vibration modes. Figure 3 shows the typical in situ Raman spectra of HFC-152a molecule in the hydrate, HFC-152a-rich liquid, and aqueous phases on the thermodynamic stability boundary at 159 MPa and 305.1 K. The asterisk indicates the contributions from sapphire window of high-pressure Raman cell. The observed Raman shifts of HFC-152a molecule in each phase are summarized in Table 2, which vibration modes are assigned based on the literature.<sup>17–19</sup> The Raman shifts of the HFC-152a molecule in the HFC-152a-rich liquid phase agree with those in the pure liquefied HFC-152a phase,<sup>17</sup> although there are slight differences in the wavenumber region higher than 2800 cm<sup>-1</sup>. The broad peak detected at 205 cm<sup>-1</sup> corresponds to the intermolecular O–O vibration (lattice mode) between water molecules in the HFC-152a hydrate. All Raman peaks of HFC-152a molecule in all phases are single at 159 MPa and 305.1 K. Even at higher pressures up to 370 MPa, every peak remains single (Figure S2 of the Supporting Information). HFC-152a molecules do not occupy the S-cage of s-I HFC-152a hydrate in a pressure range up to 370 MPa. It is well-known that the C<sub>2</sub>H<sub>4</sub>,<sup>4</sup> C<sub>2</sub>H<sub>6</sub>,<sup>5</sup> CF<sub>4</sub>,<sup>20</sup> and *c*-C<sub>3</sub>H<sub>6</sub>,<sup>6</sup> molecules oppressively occupy a part of S-cages at a pressure higher than ~5 MPa, ~20 MPa, 70 MPa, and 200 MPa, respectively. The largest van der Waals diameter of *c*-C<sub>3</sub>H<sub>6</sub> molecule is 0.58 nm, very close to the diameter of void space in M-cage. The unoccupancy of HFC-152a molecule in S-cage at a high pressure above 200 MPa implies that the size of HFC-152a molecule is slightly larger than that of *c*-C<sub>3</sub>H<sub>6</sub> molecule and HFC-152a molecule would be the largest s-I hydrate former.

Figure 4 shows the pressure dependence of the Raman shifts corresponding to the three intramolecular vibrations (relatively intensive compared with others) of HFC-152a molecules. Raman shifts of the CH<sub>3</sub> symmetric deformation ( $\nu_4$ ) and CH<sub>3</sub> rocking ( $\nu_9$ ) modes (Figure 4a,b) are almost constant in the whole pressure range of the present study, while that of the C–H symmetric stretching vibration mode ( $\nu_3$ ) (Figure 4c) exhibits weak pressure dependence (0.9 cm<sup>-1</sup>/100 MPa). The pressure dependence of HFC-152a in the M-cage is larger than those of

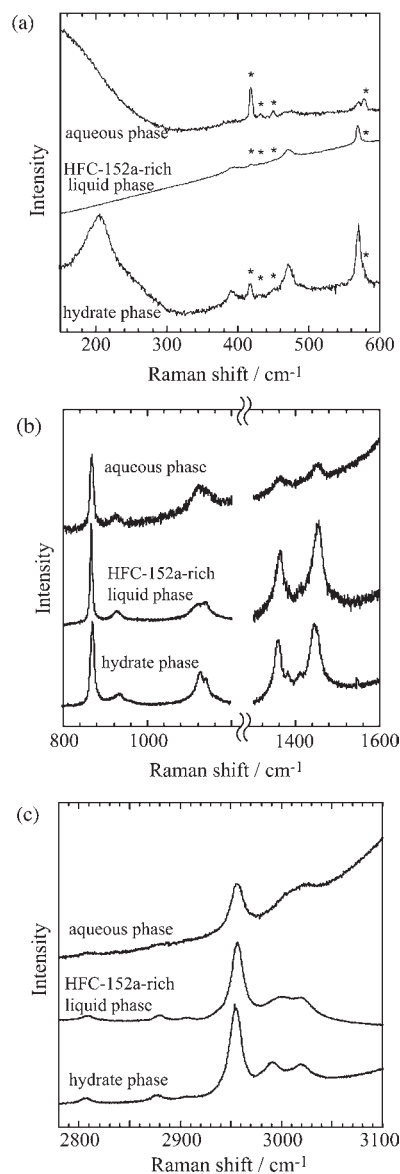


**Figure 3.** Raman spectra in the HFC-152a hydrate, HFC-152a-rich liquid, and aqueous phases at 159 MPa and 305.1 K. The peak detected around 205 cm<sup>-1</sup> in part (a) corresponds on the intermolecular O–O vibration of HFC-152a hydrate. The asterisk represents the contributions from the sapphire window. The other peaks are derived from the intramolecular vibration of the HFC-152a molecule in each phase. See Table 2 for the peak assignments.

the C–H symmetric stretching vibration mode of CH<sub>4</sub>,<sup>3</sup> C<sub>2</sub>H<sub>4</sub>,<sup>4</sup> and *c*-C<sub>3</sub>H<sub>6</sub><sup>6</sup> in M-cage of each simple hydrate. This result implies that the M-cage of the HFC-152a hydrate is constrained by the compression.

In our previous works<sup>3–6,20–24</sup> on gas hydrate crystals along the hydrate stability boundaries, the Raman spectrum corresponding to the intermolecular O–O vibration mode of water detected around 205 cm<sup>-1</sup> has been regarded as a practical sign of the clean hydrate crystal in the experimental sections. Moreover, the O–O vibration energy is very important information about the elasticity of the hydrogen-bonded water cages. The pressure dependence of the O–O vibration energy in the HFC-152a hydrate is shown in Figure 5 accompanied with our previous

**Table 2.** Summary on the Observed Raman Spectra ( $\Delta\nu$ ) of the HFC-152a Molecule in the HFC-152a Hydrate, HFC-152a-Rich Liquid, and Aqueous Phases at 159 MPa and 305.1 K

assignment <sup>a</sup>	mode <sup>a</sup>	hydrate $\Delta\nu$	HFC-152a-rich liquid $\Delta\nu$	aqueous solution $\Delta\nu$
		cm <sup>-1</sup>	cm <sup>-1</sup>	cm <sup>-1</sup>
$\nu_1$	C–H antisymmetric stretching	3019	3021	3025
$\nu_2$	C–H stretching	2989	2998	3006
$\nu_3$	C–H symmetric stretching	2954	2956	2956
$\nu_4 + \nu_5^b$		2876	2879	c
$2\nu_5^b$		2806	2808	c
$\nu_4$	CH <sub>3</sub> symmetric deformation	1446	1452	1453
$\nu_5$	C–C stretching	1409	1412	c
$\nu_{14}$	C–C–H bending	1378	c	c
$\nu_6$	C–C–H bending	1359	1361	1363
$\nu_7$	C–F stretching	1144	1137	1145
$\nu_8$	C–F stretching	1128	1114	1121
$\nu_{16}$	CH <sub>3</sub> rocking	935	927	924
$\nu_9$	CH <sub>3</sub> rocking	871	867	868
$\nu_{10}$	CF <sub>2</sub> bending	571	569	569
$\nu_{11}$	CF <sub>2</sub> wag	473	471	472
$\nu_{17}$	CF <sub>2</sub> twist	393	392	c

<sup>a</sup> From ref 19. <sup>b</sup> From ref 17. <sup>c</sup> Due to a very low signal-to-noise ratio.

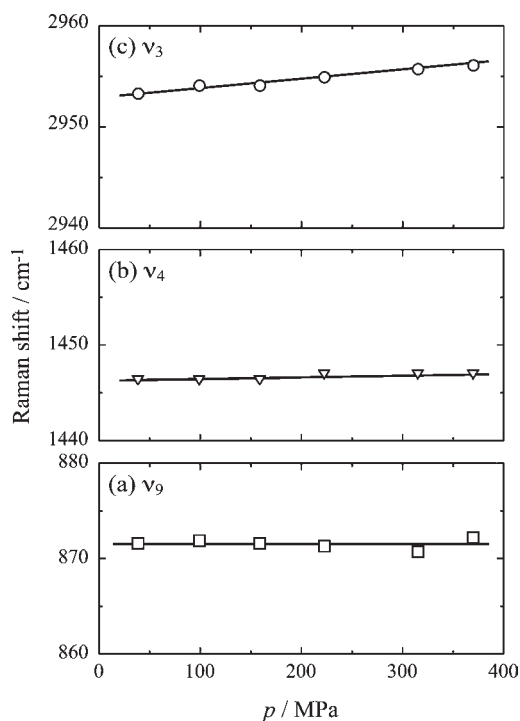


**Figure 4.** Pressure dependence of Raman shifts corresponding to the C–H symmetric stretching ( $\nu_3$ ), CH<sub>3</sub> symmetric deformation ( $\nu_4$ ), and CH<sub>3</sub> rocking ( $\nu_9$ ) modes in the HFC-152a hydrate phase along three-phase equilibrium curve of H + L<sub>1</sub> + L<sub>2</sub>.

results of other s-I hydrate systems.<sup>3–6,20–22</sup> There are two tendencies in the s-I hydrate systems; one is a strong pressure dependence of type A (CH<sub>4</sub>,<sup>3</sup> CO<sub>2</sub>,<sup>21</sup> and Xe<sup>22</sup>), and the other is a very weak pressure dependence of type B (C<sub>2</sub>H<sub>4</sub>,<sup>4</sup> C<sub>2</sub>H<sub>6</sub>,<sup>5</sup> c-C<sub>3</sub>H<sub>6</sub>,<sup>6</sup> and CF<sub>4</sub><sup>20</sup>). The stronger pressure-dependence of type A would indicate a higher shrinkage of the hydrogen-bonded cage

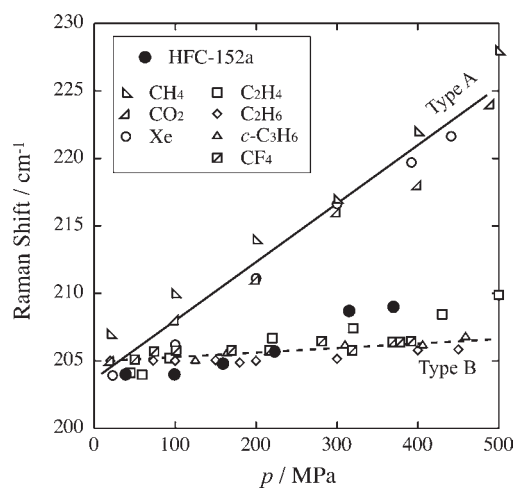


**Figure 5.** Pressure dependences of the O–O vibration energy in the s-I HFC-152a (present study), CH<sub>4</sub>,<sup>3</sup> CO<sub>2</sub>,<sup>21</sup> Xe,<sup>22</sup> C<sub>2</sub>H<sub>4</sub>,<sup>4</sup> C<sub>2</sub>H<sub>6</sub>,<sup>5</sup> CF<sub>4</sub>,<sup>20</sup> and c-C<sub>3</sub>H<sub>6</sub><sup>6</sup> hydrate systems along three-phase equilibrium curve of H + L<sub>1</sub> + L<sub>2</sub>.

or the larger free volume for the guest molecule. On the other hand, the guest molecule having a large van der Waals diameter generates the type B hydrate crystal. The O–O vibration energy in the HFC-152a hydrate shows somewhat weak pressure dependence. Raman spectra obtained in the present study reveal that the HFC-152a molecule would be the largest s-I hydrate former, and no pressure-induced structural transition occurs at a pressure up to 370 MPa. In addition, all of the S-cages in the s-I HFC-152a hydrate remains vacant even at 370 MPa.

## CONCLUSION

We measured the high-pressure phase equilibrium relations of the HFC-152a + water binary system at a pressure up to



370 MPa. In addition, in situ Raman spectra corresponding to the intermolecular vibration of water molecules of hydrate lattice and the intramolecular vibrations of the HFC-152a molecule in the single crystal of s-I HFC-152a hydrate were measured. The following important findings are obtained.

- (1) There is no structural transition in the HFC-152a hydrate at a pressure up to 370 MPa along the three-phase coexisting curve of H + L<sub>1</sub> + L<sub>2</sub>.
- (2) The HFC-152a molecule would be the largest s-I hydrate former.
- (3) No HFC-152a molecule occupies the S-cage of s-I HFC-152a hydrate even at 370 MPa.

## ■ ASSOCIATED CONTENT

**S Supporting Information.** Powder XRD pattern (Figure S1) of the HFC-152a hydrate formed at 281.0 K and 0.16 MPa (measured at 113 ± 2 K and atmospheric pressure) and the pressure dependence of Raman shifts (Figure S2) in the HFC-152a hydrate phase. This material is available free of charge via the Internet at <http://pubs.acs.org>.

## ■ AUTHOR INFORMATION

### Corresponding Author

\*Tel. and fax: +81-6-6850-6290. E-mail: [ohgaki@cheng.es.osaka-u.ac.jp](mailto:ohgaki@cheng.es.osaka-u.ac.jp).

## ■ ACKNOWLEDGMENT

We acknowledge the scientific support from the “Gas-Hydrate Analyzing System (GHAS)” of the Division of Chemical Engineering, Graduate School of Engineering Science, Osaka University (for the Raman analyses) and Rigaku Corporation (for the PXRD measurement at low temperatures). We thank Dr. Y. Egashira, Dr. H. Sato (Osaka University), and Mr. K. Nagao (Rigaku Corporation) for the valuable discussion and suggestions.

## ■ REFERENCES

- (1) Sloan, E. D.; Koh, C. A. *Clathrate Hydrates of Natural Gases*, 3rd ed.; CRC Press, Taylor & Francis Group: Boca Raton, FL, 2007.
- (2) Sum, A. K.; Burruss, R. C.; Sloan, E. D., Jr. Measurement of Clathrate Hydrates via Raman Spectroscopy. *J. Phys. Chem. B* **1997**, *38*, 7371–7377.
- (3) Nakano, S.; Moritoki, M.; Ohgaki, K. High-Pressure Phase Equilibrium and Raman Microprobe Spectroscopic Studies on the Methane Hydrate System. *J. Chem. Eng. Data* **1999**, *44*, 254–257.
- (4) Sugahara, T.; Morita, K.; Ohgaki, K. Stability Boundaries and Small Hydrate-Cage Occupancy of Ethylene Hydrate System. *Chem. Eng. Sci.* **2000**, *55*, 6015–6020.
- (5) Morita, K.; Nakano, S.; Ohgaki, K. Structure and Stability of Ethane Hydrate Crystal. *Fluid Phase Equilib.* **2000**, *169*, 167–175.
- (6) Suzuki, M.; Tanaka, Y.; Sugahara, T.; Ohgaki, K. Pressure Dependence of Small-Cage Occupancy in the Cyclopropane Hydrate System. *Chem. Eng. Sci.* **2001**, *56*, 2063–2067.
- (7) Rouher, O. S.; Barduhn, A. J. Hydrates of *iso*- and *n*-Butane and Their Mixtures. *Desalination* **1969**, *6*, 57–73.
- (8) Kubota, H.; Shimizu, K.; Tanaka, Y.; Makita, T. Thermodynamic Properties of R13 (CClF<sub>3</sub>), R23 (CHF<sub>3</sub>), R152a (C<sub>2</sub>H<sub>4</sub>F<sub>2</sub>), and Propane Hydrates for Desalination of Seawater. *J. Chem. Eng. Jpn.* **1984**, *17*, 423–429.
- (9) Brouwer, D. H.; Brouwer, E. B.; Maclaurin, G.; Lee, M.; Parks, D.; Ripmeester, J. A. Some New Halogen-containing Hydrate-formers

for Structure I and II Clathrate Hydrates. *Supramol. Chem.* **1997**, *8*, 361–367.

(10) Liang, D.; Guo, K.; Wang, R.; Fan, S. Hydrate Equilibrium Data of 1,1,1,2-tetrafluoroethane (HFC-134a), 1,1-dichloro-1-fluoroethane (HCFC-141b) and 1,1-difluoroethane (HFC-152a). *Fluid Phase Equilib.* **2001**, *187–188*, 61–70.

(11) Hashimoto, S.; Miyauchi, H.; Inoue, Y.; Ohgaki, K. Thermodynamic and Raman Spectroscopic Studies on Difluoromethane (HFC-32) + Water Binary System. *J. Chem. Eng. Data* **2010**, *55*, 2764–2768.

(12) Hashimoto, S.; Makino, T.; Inoue, Y.; Ohgaki, K. Three-Phase Equilibrium Relations and Hydrate Dissociation Enthalpies for Hydrofluorocarbon Hydrate Systems: HFC-134a, -125, and -143a Hydrates. *J. Chem. Eng. Data* **2010**, *55*, 4951–4955.

(13) Houghton, J. T.; Meira Filho, L. G.; Callander, B. A.; Harris, N.; Kattenberg, A.; Maskell, K. *Climate Change 1995, The Science of Climate Change*; Lakeman, J. A., Ed.; Cambridge University Press: Cambridge, U.K., 1995; pp 21–22.

(14) Sugahara, K.; Yoshida, M.; Sugahara, T.; Ohgaki, K. Thermodynamic and Raman Spectroscopic Studies on Pressure-Induced Structural Transition of SF<sub>6</sub> Hydrate. *J. Chem. Eng. Data* **2006**, *51*, 301–304.

(15) *Checkcell*; <http://www.ccp14.ac.uk>. Checkcell developed by Laugier, L.; Bochu, B. Laboratoire des Matériaux et du Génie Physique, Ecole Supérieure de Physique de Grenoble: Grenoble, France (accessed April 28, 2011).

(16) Dong, C. PowderX: Windows-95-based Program for Powder X-ray Diffraction Data Processing. *J. Appl. Crystallogr.* **1999**, *32*, 838.

(17) Smith, D. C.; Saunders, R. A. Infrared and Raman Spectra of Fluorinated Ethanes. IV. The Series CH<sub>3</sub>–CH<sub>3</sub>, CH<sub>3</sub>–CH<sub>2</sub>F, CH<sub>3</sub>–CHF<sub>2</sub>, and CH<sub>3</sub>–CF<sub>3</sub>. *J. Chem. Phys.* **1952**, *20*, 847–859.

(18) McNaughton, D.; Evans, C. High-Resolution FTIR Spectrum of Jet-Cooled CH<sub>3</sub>CHF<sub>2</sub>. *J. Phys. Chem.* **1996**, *100*, 9660–9664.

(19) Tai, S.; Papasavva, S.; Kenny, J. E.; Gilbert, B. D.; Janni, J. A.; Steinfeld, J. I.; Taylor, J. D.; Weinstein, R. D. Reassignment of the Vibrational Spectra of CHF<sub>2</sub>CH<sub>3</sub> (HFC-152a), CF<sub>3</sub>CH<sub>3</sub> (HFC-143a), CF<sub>3</sub>CHF<sub>2</sub> (HFC-125), and CHCl<sub>2</sub>CF<sub>3</sub> (HCFC-123). *Spectrochim. Acta, Part A* **1999**, *55*, 9–24.

(20) Sugahara, K.; Yoshida, M.; Sugahara, T.; Ohgaki, K. High-Pressure Phase Behavior and Cage Occupancy for the CF<sub>4</sub> Hydrate System. *J. Chem. Eng. Data* **2004**, *49*, 326–329.

(21) Nakano, S.; Moritoki, M.; Ohgaki, K. High-Pressure Phase Equilibrium and Raman Microprobe Spectroscopic Studies on the CO<sub>2</sub> Hydrate System. *J. Chem. Eng. Data* **1998**, *43*, 807–810.

(22) Sugahara, K.; Sugahara, T.; Ohgaki, K. Thermodynamic and Raman Spectroscopic Studies of Xe and Kr Hydrates. *J. Chem. Eng. Data* **2005**, *50*, 274–277.

(23) Sugahara, K.; Kaneko, R.; Sasatani, A.; Sugahara, T.; Ohgaki, K. Thermodynamic and Raman Spectroscopic Studies of Ar Hydrate System. *Open Thermodyn. J.* **2008**, *2*, 95–99.

(24) Sugahara, K.; Tanaka, Y.; Sugahara, T.; Ohgaki, K. Thermodynamic Stability and Structure of Nitrogen Hydrate Crystal. *J. Supramol. Chem.* **2002**, *2*, 365–368.